Tetrahedron 70 (2014) 9635–9643

Contents lists available at ScienceDirect

Tetrahedron

journal homepage: www.elsevier.com/locate/tet

Novel radical tandem 1,6-enynes thioacylation/cyclization: Au–Pd nanoparticles catalysis versus thermal activation as a function of the substrate specificity

Irene Notar Francesco [a], Justine Giauffret [a], Fabien Fontaine-Vive [a], Jennifer K. Edwards [b], Christopher J. Kiely [c], Graham J. Hutchings [b], Sylvain Antoniotti [a,*]

[a] Institut de Chimie de Nice, UMR 7272, Université Nice Sophia Antipolis – CNRS, Parc Valrose, 06108 Nice Cedex 2, France
[b] Cardiff Catalysis Institute, School of Chemistry, Cardiff University, Park Place, Cardiff CF10 3AT, United Kingdom
[c] Department of Materials Science and Engineering, Lehigh University, 5 East Packer Avenue, Bethlehem, PA 18015, USA

ARTICLE INFO

Article history:
Received 12 August 2014
Received in revised form 22 October 2014
Accepted 31 October 2014
Available online 6 November 2014

Keywords:
Cycloisomerisation
Nanocrystals
S-Nucleophile
Sustainable chemistry
Acetylthiyl radicals

ABSTRACT

We studied the reactivity of 1,6-enynes with thioacetic acid (AcSH) under either thermal conditions or in the presence of catalytic amounts of supported Au or Au–Pd nanoparticles (NPs) under mild conditions. The 1,6-enynes undergo a tandem thioacylation/cyclization to original cyclic products featuring either a homoallylic thioester function or an enol thioester function depending on the substrate topology. Interestingly, the former process was found more efficient when performed in the presence of Au–Pd NPs while the latter process can be efficiently carried out under thermal conditions (100 °C). The reaction proceeds by a radical mechanism and the presence of precious metal NPs seems to stabilize the formation of free radical intermediates, as supported by experimental and theoretical results.

1. Introduction

The need for sustainable chemical processes in the production of fine chemicals has led to innovative concepts and paradigms such as atom-, step-, and pot-economy, tandem reactions, and multicatalysis, among others.[1] Ideally, these reactions are performed with a limited energetic demand, typically at room temperature. To achieve this goal, catalysis plays a prominent role by lowering the activation energies. However, although highly efficient processes have been described with homogenous catalysts, and in particular transition metal-based catalysts, industrial applications are still in demand of scale-up capabilities for these methodologies where the economical and ecological costs cannot always be supported. On the other side, heterogeneous catalysis provides efficient recyclability of the catalysts, but has been mainly applied so far to the production of commodity chemicals. It has become desirable to design novel chemical processes taking into account the principles of green and sustainable chemistry and offering the advantages of both homogeneous and heterogeneous catalysis.[2–5]

On the boundaries of these fields, nanostructured precious metals, and notably gold nanoparticles, are expected to play a premium role.[6–8] However, while a fair amount of published research involving metal nanoparticles is dedicated to oxidation/reduction processes or coupling reactions, cycloisomerisation reactions and in particular 1,n-enynes cycloisomerisation reactions catalyzed by metal nanoparticles seem to have been neglected.[9–11] In a 2012 report, the cycloisomerisation of 1,6-enynes catalyzed by gold nanoparticles was described for the first time and intriguing differences were observed compared to the homogeneous version of the reaction.[12]

Cycloisomerisation of 1,n-enynes, combined with other reactions in tandem processes (e.g., addition of nucleophiles), provides both atom- and step economy with substantial waste formation avoided. These methods have been successfully used in the synthesis of complex scaffolds en route to valuable bio-active molecules.[13,14] Thus, tandem 1,6-enynes cycloisomerisation/nucleophile addition reactions have been developed in homogeneous catalysis with precious metal salts and complexes.[15–17] Besides the numerous examples existing with C- and *O*-nucleophiles involving cationic intermediates and exhibiting Markovnikov regioselectivities, *S*-nucleophiles have been rarely studied in these reactions. The combination of gold catalysis with the transformation of sulfur-

* Corresponding author. Fax: +33 (0) 492076151; e-mail address: sylvain.antoniotti@unice.fr (S. Antoniotti).

http://dx.doi.org/10.1016/j.tet.2014.10.077
0040-4020/

containing compounds in general have been moderately studied.[18–21] As a result, reports on enynes tandem cycloisomerisation/*S*-nucleophiles addition are limited to our best knowledge to the use of thiophenol using gold catalysis[22] or AIBN,[23] and diphenyl disulfide under single electron transfer (SET) conditions,[24] leading in both cases to enol phenyl thioethers with anti-Markovnikov selectivities (Scheme 1). In contrast, the use of AcSH as nucleophile in cyclopropene ring-opening reactions homogeneously catalyzed by electrophilic Au(I) complexes proceeds with Markovnikov selectivity following an ionic mechanism.[25] Radical reactions involving 1,6-enynes and triggered by AIBN have been reported to allow for selective cyclization in spite of multiple possible directions for the radical attack by kinetic selection of the least stable radical by 5-exo-trig ring closure.[26,27]

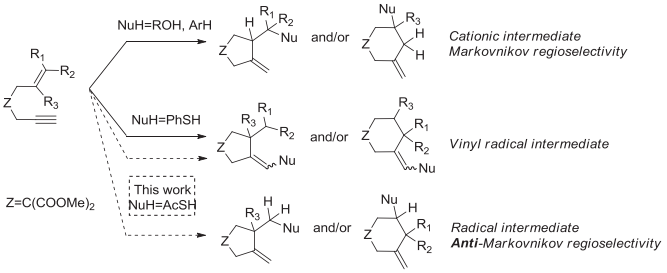

Scheme 1. Types of products and selectivities observed in tandem cyclization/nucleophile addition of 1,6-enynes.

In this context, we have been interested in studying the reactivity of 1,6-enynes and thioacetic acid in tandem thio-nucleophile addition/cyclization reactions. The effect of supported noble metal NPs on the course of the reactions was studied under mild heterogeneous conditions and compared with thermal conditions (100 °C). The particular choice of Au and Au–Pd NPs was mainly guided by the known capacity of these metals to activate π-bonds and the possible radical stabilization at the surface of Au NPs.[28,29] Even if the mechanisms involving metal nanoparticles are not yet comprehensively known, it is admitted that at the nanometric scale, atoms located at edges or corners of nanocrystals could behave as cations by electrons delocalization even at a zero oxidation state.[6,30] In regards of AcSH as sulfur transfer agent, we privileged the ease of handling and the capacity of the thioester products to be further transformed by hydrolysis or reduction, an option not offered by the existing methods involving thiophenoxyl radicals and leading to enol phenyl thioethers.

In this paper, we present our results showing that in the presence of AcSH and Au–Pd NPs, various 1,6-enynes bearing a methallyl moiety (R_1=R_2=H, R_3=Me) undergo a radical tandem thioacylation/cyclization leading preferentially to cyclic products featuring a homoallylic thioester function. With other type of 1,6-enynes (R_1, R_2=H, alkyl, aryl, R_3=H), rings with exocyclic enol thioester functions are obtained efficiently under thermal conditions following a more common route (Scheme 1).

2. Results and discussion

Precious metal NPs supported on TiO_2 were prepared by impregnation using an aqueous solution of tetrachloroauric acid, or aqueous solutions of tetrachloroauric acid and palladium(II) chloride, added simultaneously to TiO_2. The paste obtained was then dried and further calcinated at 400 °C.[31,32]

The structure and composition of Au–Pd/TiO_2 catalyst were analyzed by analytical electron microscopy. Fig. 1a shows a low magnification HAADF-STEM image in which the metal particles appear

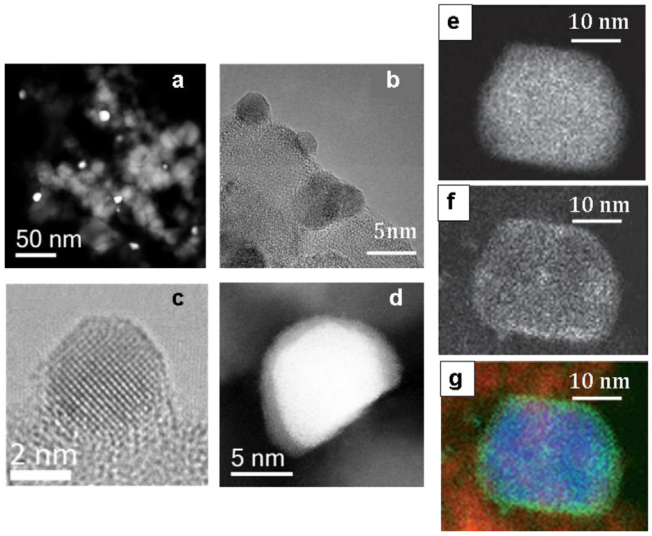

Fig. 1. Representative lower magnification (a) HAADF-STEM and (b) HR-TEM images of the impregnated Au–Pd/TiO_2 sample; (c) HRTEM image of an Au–Pd particle along an <110> zone axis showing {111}, {200 and {220}-type surface faceting; (d) An HAADF-STEM image of an individual Au–Pd exhibiting a core–shell type morphology in which the Au preferentially wets the TiO_2; (e) Au-Lα and (f) Pd-Lα XEDS elemental maps and (g)Ti (red)-Au (blue) -Pd (green) overlay map from one of the larger alloy particles confirming a definite Au-rich core/Pd-rich shell morphology.

bright against the TiO_2 particles by virtue of atomic number contrast. The Au–Pd particle size was found to vary widely between 2 and 200 nm with a mean size of 5–6 nm. The larger particles were always found to have an Au-rich composition whereas the smaller ones were invariably Pd-rich. Fig. 1b and c shows HR-TEM images of alloy particles in which the structure from the Au–Pd can be determined as FCC. The image (c) also illustrates the propensity of the particles to form low energy {111}, {200} and {220} surface facets. The HAADF-STEM image in Fig. 1d shows that the particles also have a tendency to 'wet' the TiO_2 forming a flat extended interface, which ultimately stabilizes the nanoparticles against excessive thermal sintering. The Au–Pd particle in Fig. 1d is also seen to adopt a definite core–shell morphology. Furthermore, the elemental maps acquired from a large individual particle (30 nm) presented in Fig. 1e, (f) and (g) confirm that such particles have a Pd-rich shell and Au-rich core.

Metal NPs were tested in various reaction conditions involving substrate **1a** as a model (not shown). The reactions yielded a 5-membered ring carbocycle **1b**, featuring a methylidene and a thioacetylmethyl group at the allylic position, or an exocyclic enol thioester **1c** (mostly the 5-membered ring isomer), in line with previously reported reactions involving thiol functions. CH_3CN was identified as the most adapted solvent based on yields and selectivity.

We further screened a series of NPs as possible catalysts for the reaction of **1a** at 30 °C (Fig. 2). The conversion of **1a**, measured after 2 h reaction time was 0% with Au/TiO_2, Au/CeO_2, Au/$Mg(OH)_2$, and Aurolite® (a commercial form of Au NPs/TiO_2). Gold nanoparticles supported on graphite allowed the conversion to reach 78% but a large amount of undesired **1b′** product was formed, resulting from the addition of a second AcSH molecule to **1b**. A conversion of 69% was obtained with Au–Pd alloy NPs at the remarkable 0.5 mol % metal/substrate ratio with 80% selectivity in favor of **1b** over **1c** without side product. Additional experiments at 60 °C with Au NPs/C and Au–Pd NPs/TiO_2 allowed an improvement of the conversion with the bimetallic catalyst. The stereochemistry of enol thioester **1c** was predominantly *Z* (8:2).

Control experiments were conducted with AuCl to compare with a homogeneous system, without any metal nor support (−/−), and with the support TiO_2 without NPs (−/TiO_2). With AuCl, or without any added metal, no reaction took place. With TiO_2 alone,

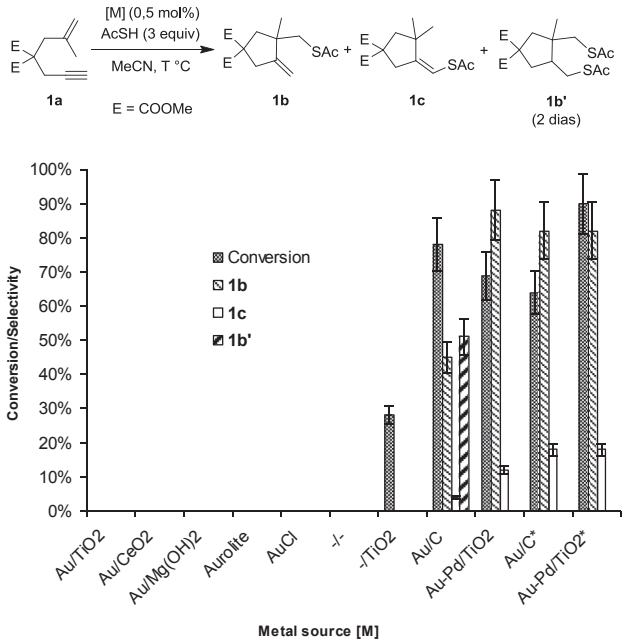

Fig. 2. Metal source screening. Substrate 0.5 mmol, AcSH 1.5 mmol, anhydrous CH_3CN, 30 °C, 2 h, N_2 atmosphere. Metal source 10 mg, titrating 5% w/w in metal excepted Aurolite (1% w/w, 50 mg). Control experiment: -/TiO_2 for the reaction with 10 mg TiO_2, –/– for the reaction without metal nor support. Reactions marked with (*) where conducted at 60 °C.

a conversion of 28% was observed but no product could be detected in the reaction medium; degradation probably occurred.

The possible leaching of cationic gold species from the NPs was evaluated by ICP-MS analysis of residual Au in the reaction mixture after 3 h with Au–Pd at 30 and 60 °C. The gold concentrations in solution were found to be 3, and 11 ppm, respectively (±2%). Such very low concentrations represent 0.0024, and 0.0089 mol % metal/substrate ratios, respectively, and could not account for the catalysis. No conversion indeed was observed with 0.5 mol % homogeneous AuCl at 30 °C and only 33% after 28 h at 60 °C (not shown).

The plot of the conversion versus the course of time for Au–Pd NPs/TiO_2 and TiO_2 alone at 30 °C confirmed the catalytic effect of as low as 0.5 mol % noble metal NPs on the reaction rate (Fig. 3). After a period of induction of a few minutes, nearly 80% of **1a** was converted in 3 h to form predominantly product **1b**. With TiO_2 alone, ca. 30% of **1a** is consumed within 25 min without the formation of detectable products, indicating that degradation or oligomerisation

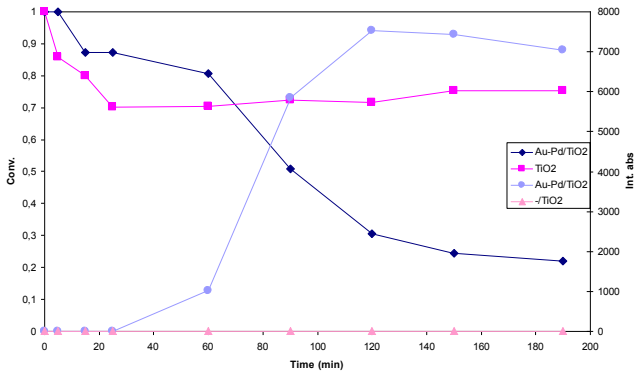

Fig. 3. Time course experiments for the reaction of **1a** (0.5 mmol) with AcSH (1.5 mmol) in CH_3CN (0.5 M) in the presence 5% w/w Au–Pd NPs/TiO_2 (10 mg, equivalent to 0.5 mol %) (◆) and TiO_2 (10 mg) (■) expressed as the conversion (primary axis). The cumulated formation of products **1b**/**1c** is also given (Au–Pd NPs/TiO_2 (●) and TiO_2 (▲), absolute integration, secondary axis). Data obtained by GC-TCD with external calibration for **1a**.

could occur. With Au–Pd NPs, prolonged reaction times at 30 °C did not allow reaching a total conversion and resulted in the slow degradation of product **1b** to polyaddition products such as **1b'**. Improved conversions and yields were however obtained in similar conditions with Au NPs/C and Au–Pd NPs/TiO_2 at 60 °C, which seemed to be the best compromise for optimizing the yield of **1b**.

The formation of **1b** as the major product was rather unexpected since thiols typically add to the alkyne terminus of enynes in the presence of radical initiators such as AIBN.[23] One might however consider that mainly data on alkyl and aryl thiols are available in the literature and that this shift of reactivity could be explained by the use of AcSH instead of RSH, exhibiting an electron-withdrawing effect on the sulfur atom.[33] Another reaction with **1a** in these conditions at 60 °C was performed using PhSH instead of AcSH. Interestingly, only a mixture of enol thioether products (*E*,*Z*)-**1c** were formed, along with their 6-membered ring analogs and doubly thioacylated products without selectivity, while **1b**-analog was not formed. The replacement of PhSH by AcSH therefore allowed a different and unprecedented reactivity of 1,6-enynes, favored in the presence of Au–Pd NPs.

The formation of **1b** selectively from the reaction of **1a** with AcSH in the presence of Au–Pd NPs/TiO_2 was thus confirmed and improved to 90% conversion upon heating at 60 °C (Table 1, entry 1).

Table 1
Tandem reactions of **1a**–**7a**[a]

Entry	Substrate	[M]	Time	Conv.	Products, selectivity[b]
1	 **1a**	Au–Pd/TiO_2	28 h	90%	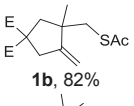 **1b**, 82% 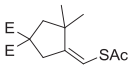 **1c**, 18%
2	 **2a**	Au–Pd/TiO_2	24 h	29%	Inseparable mixture of **2a**–**c**, and polyaddition products
3	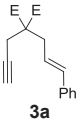 **3a**	Au–Pd/TiO_2	24 h	30%	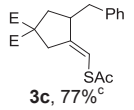 **3c**, 77%[c]
4	 **4a**	Au/C	6 h	29%	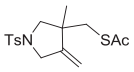 **4b**, 100%
5	**4a**	Au–Pd/TiO_2	7.5 h	65%	**4b**, 100%
6	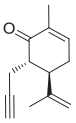 **5a**	Au–Pd/TiO_2	24 h	77%	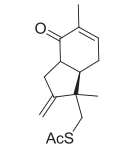 **5b**, 65% (67:33) 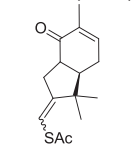 **5c**, 21% (75:25) **5b'**, 14%

(*continued on next page*)

Table 1 (*continued*)

Entry	Substrate	[M]	Time	Conv.	Products, selectivity[b]
7[d]	**5a**	Au–Pd/TiO_2	24 h	100%	**5b**, 45% **5c**, 46% **5b′**, 9%
8	 **6a**	Au–Pd/TiO_2	5 h	91%	**6b**, 78% (2 dias 1:1) **6c**, 22%
9	 **7a**	Au–Pd/TiO_2	9 h	40%	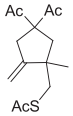 **7b**, 100%

[a] Conditions: substrate (0.5 mmol, E=COOMe), AcSH (1.5 mmol) in anhydrous and degassed acetonitrile (1 mL), 60 °C, N_2. [M] 10 mg (0.5 mol % metal). Reactions were quantitative.
[b] Based on isolated yields.
[c] Along with 23% of double addition product from **3a**.
[d] Reaction performed at 30 °C.

The unusual reactivity observed leading to original structures such as **1b** prompted us to examine the behavior of other substrates under these reaction conditions (Table 1). A first set of changes was made on the double bond. With substrate **2a**, the conversion remained modest and a mixture of cyclized products was obtained, including polyaddition products (entry 2). Substrate **3a** delivered selectively the cyclic product **3c**, but the conversion remained moderate (entry 3).

A second set of changes from **1a** was made on the tether, either by introducing a tosylamine moiety as in **4a** or using a carvone-derived substrate such as **5a**. Substrate **4a** with both methallyl and propargyl substituents was cyclized in the presence of Au/C and Au–Pd/TiO_2 similarly to **1a** leading selectively to product **4b**, with 29 and 65% conversion, respectively (entries 4, 5). Again, bimetallic Au–Pd NPs were superior to their monometallic counterpart and we decided to focus on this catalyst.

Substrate **5a**, derived from carvone, was converted into the corresponding thioester **5b**, obtained in the form of a mixture of diastereomers (2 majs. 67:33), in 77% conversion and 65% selectivity in the presence of Au–Pd/TiO_2 (entry 6). As a side product, the doubly thioacetylated product **5b′** was formed with 14% selectivity by the formal addition of AcSH to **5b**. With the same catalyst at 30 °C, the conversion was improved up to 100% but the selectivity in favor of **5b** decreased (entry 7). It is worth mentioning that a side reaction was observed consisting in the addition to AcSH to acetonitrile, favored by the application of higher temperatures. This reaction might be limited at 30 °C, accounting for the higher conversion due to a higher AcSH concentration in the reaction medium. Finally, we modified the electron-withdrawing groups E on the tether with substrates **6a** and **7a**, derived from ethyl acetoacetate and pentane-2,4-dione, respectively. In the presence of Au–Pd NPs, the cyclized products **6b** and **7b** were formed with good to excellent selectivities and moderate to excellent conversions (entries 8, 9).

Returning to malonate derivatives related to **1a**, we tested substrates **8**–**12a**, featuring variations on the alkenyl side chain with di- and trisubstituted double bonds with NPs in acetonitrile (Table 2). In general, with this type of substrates, we observed a reactivity shift towards the formation of enol thioesters **8**–**12c** with good to excellent selectivities (60–100%) instead of homoallylic thioesters **8**–**12b**, albeit with modest conversion (17–61%).

The stereochemistry of cyclic enol thioesters **8**–**12c** was found to be predominantly *Z* or predominantly *E* depending on the substitution on the olefinic side chain. Substrates with small substituents such as H, or Me yielded mostly the *Z* isomer (cases of **2a**, **8a**, and **9a**), while bulky substitution at this position yielded mostly the *E* isomer (cases of **3a**, **10a**, **11a** and **12a**).

Table 2
Tandem reactions in CH_3CN[a]

Entry	Substrate	Conv.[b]	Products, selectivity[b]
1	 **8a**	17%	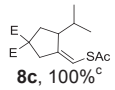 **8c**, 100%[c]
2	 **9a**	24%	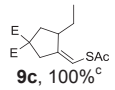 **9c**, 100%[c]
3	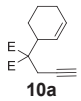 **10a**	61%	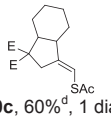 **10c**, 60%[d], 1 dia
4	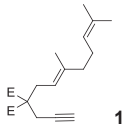 **11a**	47%	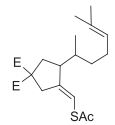 **11c**, 100%[e], 2 dias, 1:1
5	 **12a**	17%	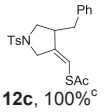 **12c**, 100%[c]

[a] Conditions: substrate 0.5 mmol (E=COOMe), AcSH (3 equiv), anhydrous and degassed CH_3CN, 60 °C, 24 h, nitrogen atmosphere. Au–Pd/TiO_2 (10 mg, 0.5 mol % metal). Reactions were quantitative.
[b] Based on isolated yields.
[c] Predominantly *Z*.
[d] Predominantly *E*. Along with 17% of **10b** (2 dias, 1:1) and 23% of doubly thioacylated product.
[e] Predominantly *E*. Trace amount of doubly thioacylated product were formed.

The position of the SAc group in the products attached in an anti-Markovnikov fashion suggested that radical reactions could be involved. This hypothesis was probed by running the reaction of Fig. 2 at 60 °C in the presence of TEMPO (0.2 equiv). Using either Au NPs or Au–Pd NPs, no conversion of **1a** was observed after 28 h in the presence of the radical scavenger. Even if TEMPO is not supposed to interact with thiyl radicals, it could react once a carbon-centered radical is formed upon the attack of the thiyl radical and therefore shut down the radical propagation. The reaction was conducted in the absence of light, and no significant differences were observed in terms of conversion and products selectivity. In the presence of AIBN (20 mol %) instead of metal nanoparticles in our conditions (Table 1), only 19% conversion was observed after 2 h (to be compared to 90% with Au–Pd NPs) but the results in terms of yield and selectivity towards **1b** could be reproduced after 24 h. No difference was observed when running the reaction in the presence of both 20 mol % AIBN and 0.5 mol % Au–Pd NPs.

A radical-based mechanism has thus to be considered and a couple of additional experiments were performed. It is known that Au NPs have the ability to oxidize thiols to disulfides in the presence of O_2. In our cases, AcSH could be converted to AcSSAc, further homolytically cleaved to generate AcS• by heating or at the precious metal surface. Dimeric AcSSAc could indeed be identified in the reaction mixture by GC/MS but could not be isolated (see SI). Hence a reaction with **3a** was carried out with PhCOSH and at the end of the reaction, the thiobenzoylated analog of **3c** was formed, and $(PhCOS)_2$ was isolated by column chromatography. The dimer

was further engaged in a reaction with both fresh substrate and NPs but no conversion was observed, ruling out the hypothesis of BzSSBz as an active species in our conditions. With AcSK or with AcSH in the presence of Et_3N at 60 °C, no conversion was observed after 18 and 22 h of heating, respectively. Having demonstrated that neither AcSSAc or AcS^- were active in these reactions, we had to consider unmodified AcSH as the active species. Molecule-assisted homolysis (MAH)[34] could also be of concern here, allowing the initial radical addition of AcSH to a multiple bond, which could be followed by a radical chain transfer involving AcS•. It is worth noting that in our case, the radical reaction could be conducted without using AIBN or irradiation, as it is typically the case in reactions involving thiyl radicals,[35] and only 0.5 mol % of Au–Pd NPs at 30 °C were enough to trigger the reaction (Figs. 1 and 2). At elevated temperatures, the S–H bond of AcSH (dissociation energy: 88 kcal/mol) is likely to be homolytically cleaved.[36] This hypothesis was probed when substrate **1a**, **13a**, and **14a** were treated by AcSH in toluene at 100 °C in the absence of catalyst. In these conditions, the anti-Markovnikov products **13d** and (*E*/*Z*)-**14d** were obtained quantitatively in 3 h. These experiments showed that upon heating, both the double and the triple bonds could be attacked by AcSH. This attack led selectively and quantitatively to the corresponding addition products, thereby suggesting that one or the other moiety within substrate **1a** could react. These thermal conditions however failed to lead selectively to **1b**, suggesting a role of NPs in the cyclization process (Scheme 2).

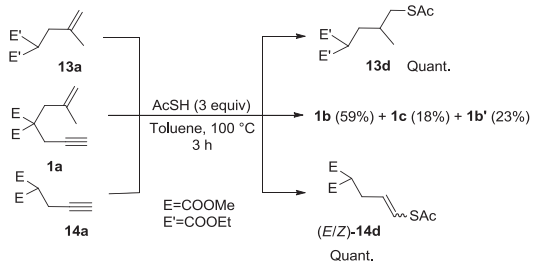

Scheme 2. Addition of AcSH to C–C multiple bonds without initiators or additives.

If the procedure involving Au–Pd NPs in acetonitrile allowed the best results with terminal disubstituted double bonds (Table 1), the modest conversion rates observed with other substrates, leading to type **c** products (Table 2), prompted us to use toluene as the solvent under thermal conditions by heating the reaction at 100 °C (Table 3).

Table 3
Tandem reactions under thermal conditions in toluene[a]

Entry	Substrate	Conversion	Products, yields
1	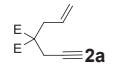 **2a**	100%	**2b**, 21% **2c**, 40% **2a'**, 20%[b]
2	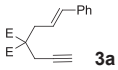 **3a**	100%	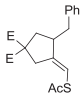 **3c**, 73%
3	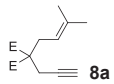 **8a**	85%	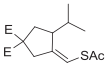 **8c**, 79%
4	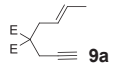 **9a**	100%	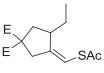 **9c**, 48%[c]

(*continued*)

Table 3 (*continued*)

Entry	Substrate	Conversion	Products, yields
5	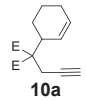 **10a**	100%	 **10c**, 73%, 1 dia
6	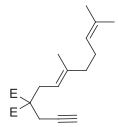 **11a**	100%	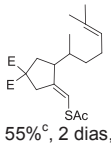 **11c**, 55%[c], 2 dias, 1:1

[a] Conditions: substrate 0.5 mmol (E=COOMe), AcSH (3 equiv), anhydrous and degassed toluene, 100 °C, nitrogen atmosphere, 1–4 h reaction time.
[b] Product **2a'** is formed upon the double addition of AcSH to **2a**.
[c] Together with small amounts of non cyclized thioacylated product.

This change was rewarded by the formation of enol thioester products **c** in short reaction times and high conversions. Only in the case of **2a**, product **2c** was formed in 40% yield, along with polyaddition products (entry 1). However, with substrates **3a** and **8a**, enol thioester products **3c** and **8c** were formed in 73–79% yields with good to excellent conversions (entries 2, 3). Substrate **9a** yielded **9c** in a modest 48% (entry 4). Cyclohexenyl substituted substrate **10a** delivered diastereoselectively *cis*-fused cyclized product **10c** in 73% yield (entry 5). Geranyl substituted substrate **11a** was converted to **11c** in 55% as an equal mixture of diastereomers (entry 6).

Although the reactivity of methallyl-bearing substrates towards the formation of type **b** products required the presence of Au–Pd NPs at lower temperatures, an alternative procedure for the formation of type **c** products by thermal activation could thus be proposed.

A working mechanism was envisaged to explain the formation of products of type **b** and **c** (Scheme 3).

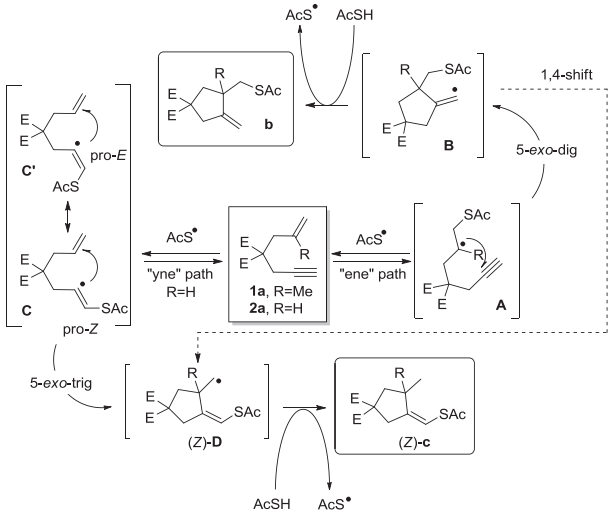

Scheme 3. Hypothetical mechanism accounting for the product selectivity during the propagation of the radical reaction. E=COOMe.

NPs could be involved in generation of AcS• at low temperature (*e.g.*, 30 °C), in radicals stabilization during the course of the reaction, and in radical transfer termination. Radical stabilization at the surface of Au NPs has been indeed recently invoked in the cyclotrimerisation of electron-deficient alkynes in the presence of molecular oxygen[28] and with Au–Pd NPs in the oxidation of toluene by TBHP.[29]

For R=Me such as with substrate **1a**, the anti-Markovnikov attack of AcSH following the 'ene' path, favored with R≠H, leads

to intermediate **A**, featuring a stabilized tertiary radical, and further undergoing 5-*exo*-dig cyclization to intermediate **B** further leading to product **1b** after H• abstraction from AcSH, liberating AcS•. At this point, we could not discard that **B** undergoes a 1,4-shift of the thioacetyl group to intermediate **D**, the Z stereochemistry being favored also in that case. While the slightly electrophilic alkyl thiyl radicals generally react preferentially with the triple bond of enyne substrates,[33] it is plausible that the action of AcS•, of higher electrophilicity, is oriented towards the attack of the double bond of **1a**, both electronically enriched and sterically accessible by the substitution with donating groups at the β-position.

With R=H as in substrate **2a**, the attack of AcSH occurs predominantly on the triple bond yielding **C**, and the 5-*exo*-trig cyclization gives rise to intermediate (*Z*)-**D** further reduced to product (*Z*)-**2c** after H• abstraction from AcSH, liberating AcS•. The stereochemistry is probably defined by the relative stability of **C** and **C′** and the energy of cyclization **C**→**D**; with substrates featuring a low substitution degree of the double bond like **2a**, the selection of the more stable isomer **C**, exhibiting minimized steric hindrance leads to (*Z*)-**D**. With substrates bearing bulky substituents on the olefinic side chain, the less stable isomer **C′** is most likely involved to minimize the repulsion during the ring closure and yields products with an *E* stereochemistry (see Tables 2 and 3). The activity of noble metal NPs, and particularly Au–Pd alloy NPs, seems to increase the initial conversion rate of the starting 1,6-enynes and to control the addition of AcSH, limiting the formation of products of type **a′** or **b′**.

The possible role of NPs through a template effect for the reaction was investigated by molecular modeling comparing reaction pathways A→B (with E=H) and energies in the gas phase and on a model gold surface (DFT studies). As anticipated, the presence of a surface resulted in a stabilization of ca. 50.2 kJ/mol for the cyclized radical **B**, while the energy barrier to reach $\mathbf{TS_{AB}}$ was calculated to be 37.9 kJ/mol in the gas phase and 34.1 kJ/mol on the surface (Fig. 4).

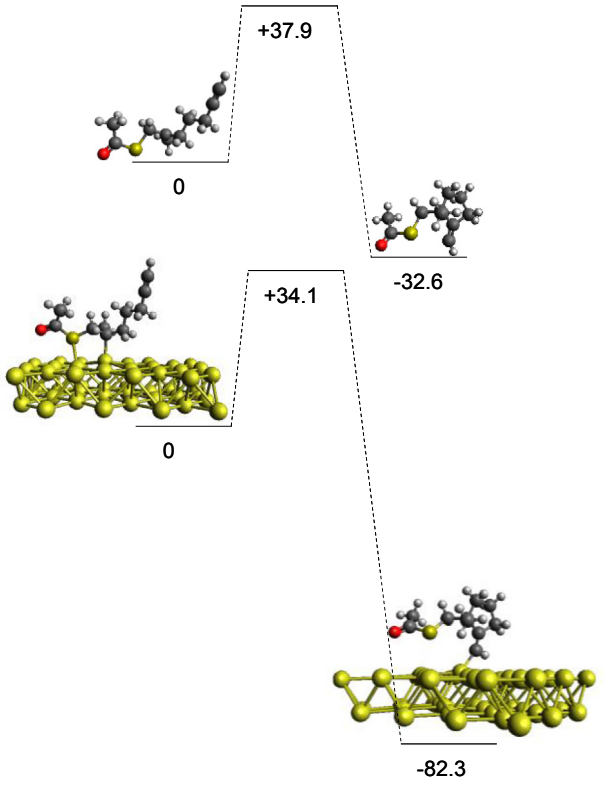

Fig. 4. Optimized geometries and energies (kJ/mol) of the reaction **A**→**B** (E=H) in the gas phase (top) and on a gold surface (bottom). See Supplementary data for calculation details.

Interestingly, while intermediate **A** featuring a sp3-carbon centered radical is attached through to the surface both by the sulfur atom and the radical, intermediate **B** is only attached by the sp2-carbon centered radical, which suggests a stronger interaction with the surface accounting for the selectivity. With respect to the bond lengths, Au–S is of 2.63 Å in **A** and 3.18 Å in **B** and Au–C• is 2.24 Å in **A** and 2.08 Å in **B**. Binding energies between both **A** and **B** on the gold surface were calculated to be −119.6 and −165.6 kJ/mol, respectively. If substrate **1a** reacts through the triple bond first, leading eventually to **1c**, an energy barrier of 148.1 kJ/mol is necessary for the cyclization to proceed on the surface, leading to a cyclic product at −69.1 kJ/mol. The same reaction in the gas phase requires only 12.2 kJ/mol and leads to the cyclic product at −96.9 kJ/mol.

These theoretical results support the hypothesis that a radical stabilization on the precious metal surface of the nanoparticle enables an equilibrium shift in favor of the formation of the cyclized product **1b** with respect to **1c**. This stabilization phenomenon, and the possible role of NPs in the homolytic cleavage of the sulfhydryl bond of AcSH, could account for the overall improved yields observed in the presence of Au and Au–Pd NPs with enyne substrates bearing a terminal disubstituted double bond.

3. Conclusions

In summary, we described the reactivity of 1,6-enynes in the presence of AcSH and small amounts of supported Au or Au–Pd NPs under mild conditions. 1,6-Enynes featuring a methallyl side chain underwent an anti-Markovnikov tandem thioacylation/cyclization to original cyclic products bearing a homoallylic thioester function. The heterogeneously catalyzed reaction proceeded at atmospheric pressure and at temperature as low as 30 °C and did not require the use of additives, radical initiators or ligands. A radical mechanism has been proposed that is supported by preliminary theoretical studies. This involves the unusual electrophilic AcS• radical, with the role of NPs to stabilize the radical ground state in favor of the formation of cyclized products. An alternative thermal procedure was proposed for substrates leading to enol thioester products.

4. Experimental section

^{1}H NMR and ^{13}C NMR spectra were recorded on BRUCKER AC 200 (200 MHz) and BRUCKER AVANCE 500 (500 MHz). ^{1}H NMR spectra are reported as follows: chemical shift in ppm (δ) relative to the chemical shift of $CDCl_3$ at 7.26 ppm, integration, multiplicities (s=singlet, d=doublet, t=triplet, q=quartet, m=multiplet and br=broadened), and coupling constants (Hz). ^{13}C NMR spectra reported in ppm (δ) relative to $CDCl_3$ at 77.16 ppm. The stereochemistry of the enol thioester double bonds was determined by comparison of the ^{13}C chemical shifts at the allylic positions.

Column chromatography was carried out employing silica gel (spherical, neutral, 63–200 um, Geduran Si 60, Merck KGaA).

Samples of Au–Pd/TiO_2 catalysts were prepared for TEM/STEM analysis by dry dispersing the catalyst powder onto a holey carbon TEM grid. High resolution transmission electron microscopy (HR-TEM) and high-angle annular dark field (HAADF) imaging experiments were carried out using a 200 kV JEOL 2200FS (scanning) transmission electron microscope equipped with a CEOS aberration corrector. XEDS spectrum images were acquired on a 300 kV VG HB 603 STEM equipped with a Nion Inc. aberration corrector. Multivariate statistical analysis (MSA) of the XEDS data cubes was carried out utilizing the MSA plug-in for Digital Micrograph.

GC-TCD analysis were carried out using a Shimadzu 2010 plus gas chromatograph, under the following operation conditions: vector gas, He; injector temperature, 250 °C; detector temperature, 210 °C at 60 mA; split ratio, 1/20; total flow, 22,5 mL/min;

Phenomenex Zebron ZB5MS column, polydimethylsiloxane (10 m, inside diameter 0.10 mm, film thickness 0.10 μm); temperature program, 80–200 °C at 10 °C/min and 200 °C for 8 min.

GC–MS analysis were performed by using a Shimadzu QP2010 gas chromatograph (conditions: carrier gas, He; injector and detector temperatures, 250 °C; injected volume, 0.5 μL; split ratio, 1/100; (pressure, 180 kPa); SLB-5ms capillary column (thickness: 0.25 mm, length: 30 m, inside diameter: 0.25 mm); temperature program, 60–250 °C at 2 °C/min, and 250 °C for 10 min, coupled to a mass selective detector. Mass spectra were obtained by electron ionization at 70 eV, *m*/*z* 35–400, source temperature 250 °C; only the most abundant ions are given.

High resolution mass spectrometry (HRMS) was performed at ERINI platform (Grasse, FRANCE) using a Waters APGC coupled with a Waters Xevo G2 QTOF spectrometer.

Inductively-coupled plasma mass spectrometry (ICP-MS) was performed using a Perkin–Elmer Elan DRCII spectrometer.

Starting 1,6-enynes were prepared by conventional procedures of alkylation of dialkyl malonate or *N*-tosylamine in the presence of K_2CO_3/DMF or NaH/THF.[37] Substrate **5a** derived from (*R*)-carvone was prepared in the presence of LDA/THF following a procedure adapted from the literature.[38] Precious metal NPs preparation and characterization have been previously reported.[31,32]

General procedure for the tandem cyclization/thioacylation of 1,6-enynes. In a Schlenk tube, the substrate (0.5 mmol), supported NPs (2.5 μmol of metal, 10 mg of material) and anhydrous and degassed solvent (1 mL) are introduced under a nitrogen atmosphere. AcSH (1.5 mmol, 108 μL) is then added, the tube close with a septum and mounted with a N_2 balloon. The mixture is stirred at the desired temperature. After completion of the reaction, monitored by TLC or GC-TCD analysis of samples withdrawn from the reaction medium, the mixture is filtered through a pad of silica gel (fluent: diethyl ether). After concentration and purification by flash chromatography over silica gel (petroleum ether/Et_2O 95/5 to 80/20) the cyclized products are obtained, typically in the form of colorless or pale yellow oils, except **12c** obtained as a solid.

Spectral data of the main products are given below. Detailed data and spectra for the compounds presented in this paper and calculation details are provided in Supplementary data.

Dimethyl 3-(acetylthiomethyl)-3-methyl-4-methylenecyclopen-tane-1,1-dicarboxylate **1b**. ^{1}H NMR ($CDCl_3$, 200 MHz): δ 4.97 (1H, *t*, *J*=2 Hz); 4.85 (1H, *t*, *J*=2 Hz); 3.72–3.73 (6H, m); 3.07 (2H, m); 3.07 (1H, d, *J*=14 Hz); 2.91 (1H, d, *J*=14 Hz); 2.39 (1H, d, *J*=14 Hz); 2.33 (3H, s); 2.27 (1H, d, *J*=14 Hz); 1.10 (3H, s). ^{13}C NMR ($CDCl_3$, 50 MHz): δ 195.49; 172.38; 154.91; 107.32; 57.61; 53.00; 45.50; 41.38; 40.07; 30.76; 26.64. MS (EI, 70 eV) 300(0.2) [M^+•], 257(3), 227(14), 224(20), 211(26), 197(8), 179(49), 164(22), 151(85), 137(10), 123(27), 105(25), 91(58), 77(22), 59(34), 43(100). HRMS calculated for $C_{14}H_{21}O_5S$ (MH^+) 301.1110; found 301.1112. Δ=0.7 ppm.

(*Z*)-Dimethyl 4-(acetylthiomethylene)-3,3-dimethylcyclo-pentane-1,1-dicarboxylate (*Z*)-**1c**. ^{1}H NMR ($CDCl_3$, 200 MHz): δ 6.29 (1H, *t*, *J*=3 Hz); 3.73 (6H, s); 3.04 (2H, d, *J*=3 Hz); 2.30–2.40 (5H, m); 1.12 (6H, s). ^{13}C NMR ($CDCl_3$, 50 MHz): δ 192.11; 172.40; 172.40; 152.11; 107.49; 58.07; 53.12; 53.12; 48.43; 43.78; 39.40; 30.70; 29.30; 29.30. MS (EI, 70 eV) 300(2) [M^+•]; 269(1), 258(7), 240(5), 225(1), 198(42), 183(5), 165(7), 151(7), 139(9), 121(6), 105(15), 93(8), 91(12), 79(10), 77(10), 59(22), 43(100). HRMS calculated for $C_{14}H_{21}O_5S$ (MH^+) 301.1110; found 301.1114. Δ=1.3 ppm.

(*Z*)-Dimethyl 3-((acetylthio)methylene)-4-methylcyclo-pentane-1,1-dicarboxylate (*Z*)-**2c**. ^{1}H NMR ($CDCl_3$, 200 MHz): δ 6.27 (1H, ddd, ^4J=4.8 Hz, ^4J=2.4 Hz, $^4J\sim$0 Hz); 3.72 (6H, s); 2.36 (3H, s) 2.25–3.11 (4H, m); 1.66–1.84 (1H, m); 1.17 (3H, d, *J*=6 Hz). ^{13}C NMR (50 MHz, $CDCl_3$) δ 192.16; 172.04; 171.91; 148.12; 107.87; 58.46; 53.05; 52.99; 42.44; 39.46; 38.78; 30.67; 17.69. MS (EI, 70 eV). HRMS calculated for $C_{13}H_{19}O_5S$ (MH^+) 287.0953; found 287.0945. Δ=2.8 ppm.

(*E*)-Dimethyl 3-((acetylthio)methylene)-4-benzylcyclo-pentane-1,1-dicarboxylate (*E*)-**3c**. ^{1}H NMR ($CDCl_3$, 200 MHz): δ 7.39–7.22 (5H, m); 6.46 (1H, ddd, ^4J=4.8 Hz, ^4J=2.4 Hz, $^4J\sim$0 Hz); 3.74 (3H, s); 3.23–3.00 (4H, m); 2.61–2.40 (1H, m); 3.77(3H, s); 2.59 (1H, dd, ^2J=13.2 Hz, ^3J=8.4 Hz); 2.43 (3H, s); 1.94 (1H, dd, ^2J=13 Hz, ^3J=10.4 Hz). ^{13}C NMR (50 MHz, $CDCl_3$) δ 191.90; 171.76; 146.20; 139.62; 128.93; 128.53; 126.32; 108.92; 58.32; 52.97; 52.94; 45.14; 39.99; 39.87; 39.78; 30.60. MS (EI, 70 eV) 286(19) [M]$^{\bullet+}$, 271(4), 228(3), 226(31), 211(10), 197(9), 169(43), 137(31), 109(9), 91(80), 65(16), 59(15), 43(100). HRMS calculated for $C_{19}H_{23}O_5S$ (MH^+) 363.1275; found 363.1266. Δ=2.5 ppm.

S-(3-Methyl-4-methylene-1-tosylpyrrolidin-3-yl)methyl ethanethioate **4b**. ^{1}H NMR ($CDCl_3$; 200 MHz): δ 7.69 (2H; d; *J*=8 Hz); 7.33 (2H; d; *J*=8 Hz); 4.92 (1H; bt; ^4J=2 Hz); 4.90 (1H; bt; ^4J=2 Hz); 4.00–3.75 (2H; m); 3.17 (1H; d; ^2J=10 Hz); 3.05 (1H; d; ^2J=13 Hz); 2.95 (1H; d; ^2J=10 Hz); 2.89 (1H; d; ^2J=13 Hz); 2.43 (3H; s); 2.30 (3H; s); 1.08 (3H; s). ^{13}C NMR ($CDCl_3$; 50 MHz): δ 194.91; 176.62; 150.34; 143.85; 132.64; 129.80; 127.91; 107.28; 58.55; 52.22; 45.90; 37.10; 30.62; 23.17; 21.64. MS (EI; 70 eV) 339(0) [M^+•], 296(4), 264(1), 250(56), 184(45), 155(28), 142(29), 108(31), 94(43), 91(100), 67(14), 65(26), 53(8), 43(56).

1,5-Dimethyl-2-methylene-4-oxo-2,3,3a,4,7,7a-hexahydro-1H-inden-1-yl)methyl) ethanethioate **5b** (diastereomeric mixture, major). ^{1}H NMR ($CDCl_3$, 200 MHz): δ 6.58–6.76 (1H, m); 5.03–4.93 (1H, m); 4.78–4.85 (1H, m); 3.25 (1H, d, ^2J=13.8 Hz); 2.95 (1H, d, ^2J=13.8 Hz); 2.34 (3H, s); 2.75–1.18 (6H, m); 1.75 (3H, s); 1.05 (3H, s). ^{13}C NMR (50 MHz, $CDCl_3$) mixture with **5c** δ 201.68; 201.42; 195.60; 195.37; 144.19; 143.92; 143.68; 135.87; 135.81; 53.98; 51.38; 51.13; 50.88; 49.59; 49.02; 46.50; 45.27; 45.18; 45.12; 37.01; 36.23; 31.69; 30.86; 30.79; 30.74; 30.50; 30.34; 30.22; 28.90; 27.97; 22.97; 15.95; 15.77; 15.39. MS (EI, 70 eV) major diastereomer 264(1) [M^+•]; 221(17), 204 (5), 188 (14), 175(52), 159(16), 147(21), 121(18), 105(21), 91(37), 77(27), 65(14), 53(20), 43(100).

1,1,5-Trimethyl-4-oxo-3a,4,7,7a-tetrahydro-1H-inden-2(3H)-yli-dene)methyl) ethanethioate **5c** (major isomer, ratio *E*/*Z* not determined). ^{1}H NMR ($CDCl_3$, 200 MHz): δ 6.58–6.76 (1H, m); 6.30–6.37 (1H, m); 2.75–1.18 (6H, m); 2.38 (3H, s); 1.75 (3H, s); 1.17 (3H, s); 0.96 (3H, s). ^{13}C NMR (50 MHz, $CDCl_3$) mixture with **5b** δ 201.68; 201.42; 195.60; 195.37; 144.19; 143.92; 143.68; 135.87; 135.81; 53.98; 51.38; 51.13; 50.88; 49.59; 49.02; 46.50; 45.27; 45.18; 45.12; 37.01; 36.23; 31.69; 30.86; 30.79; 30.74; 30.50; 30.34; 30.22; 28.90; 27.97; 22.97; 15.95; 15.77; 15.39. MS (EI, 70 eV) major isomer 264(7) [M^+•]; 222(6), 189 (61), 173(31), 161(4), 145(15), 133(9), 121(17), 113(9), 105(13), 99(20), 91(22), 77(16), 43(100). HRMS calculated for $C_{15}H_{20}O_2S$ (M^+) 264.1184; found 264.1171. Δ=4.9 ppm.

1,2-Bis(acetylthiomethyl)-1,5-dimethyl-3,3a,7,7a-tetrahydro-1H-inden-4(2H)-one **5b′** (diastereomeric mixture, 2 majs): ^{1}H NMR ($CDCl_3$, 200 MHz): δ 6.53–6.77 (1H, m); 2.31 (6H, s); 3.27–1.53 (11H, m); 1.76 (3H, s); 1.01 (3H, s). ^{13}C NMR (50 MHz, $CDCl_3$) δ 201.68; 201.42; 195.82; 195.60; 195.42; 195.38; 144.20; 143.69; 135.91; 135.86; 51.43; 51.18; 50.93; 49.63; 49.07; 46.54; 45.31; 45.17; 37.05; 36.27; 31.73; 30.89; 30.83; 30.78; 30.54; 30.26; 28.94; 28.01; 27.12; 23.01; 15.98; 15.80; 15.42. MS (EI, 70 eV) 340(0.74) [M^+•]; 298(3), 265 (6), 255(9); 222 (4), 207(3), 189 (16),175(13), 147(9), 121(46), 105(8), 91(13), 77(19), 55(6), 43(100). HRMS calculated for $C_{17}H_{25}O_3S_2$ (M^{H+}) 341.1245; found 341.1241. Δ=1.2 ppm.

Ethyl 1-acetyl-3-((acetylthio)methyl)-3-methyl-4-methylene-cyclopentanecarboxylate **6b** (2 diastereomers, 1:1). ^{1}H NMR ($CDCl_3$, 200 MHz): δ 4.98–4.87 (2H, bm); 4.87–4.73 (2H, bm); 4.18 (2H, t, ^3J=7.2 Hz); 4.17 (2H, t, ^3J=7.2 Hz); 3.12–2.93 (6H, m); 2.88 (1H, d, ^2J=13.6 Hz); 2.86 (1H, d, ^2J=13.4 Hz); 2.42–2.08 (4H, m); 2.314 (3H, s); 2.31 (3H, s); 2.13 (6H, s); 1.24 (3H, t, ^3J=7 Hz); 1.23 (3H, t, ^3J=7.2 Hz); 1.10 (3H, s); 1.06 (3H, s). ^{13}C NMR (50 MHz, $CDCl_3$)

δ 203.09; 195.48; 195.40; 172.62; 172.55; 154.92; 154.79; 107.17; 107.10; 64.34; 64.01; 61.95; 61.87; 45.58; 45.50; 44.00; 43.94; 39.94; 39.76; 39.50; 30.69; 26.63; 26.33; 26.22; 26.05; 14.08. MS (EI; 70 eV) diastereomer 1 298(0) [M$^{+\bullet}$], 256(6), 237(1), 210(12), 191(3), 179(2), 167(14), 163(3), 149(5), 135(23), 121(8), 107(5), 93(14), 77(6), 65(3), 43(100). Diastereomer 2 298(0) [M$^{+\bullet}$], 256(5), 238(1), 210(13), 191(3), 179(2), 167(14), 163(3), 149(5), 135(18), 121(10), 107(6), 105(4), 93(14), 91(10), 79(4), 77(6), 65(3), 43(100).

S-((4,4-diacetyl-1-methyl-2-methylenecyclopentyl)methyl)-ethanethioate **7b**. ^{1}H NMR ($CDCl_3$, 200 MHz): δ 4.94 (1H, t, ^4J=2 Hz); 4.79 (1H, t, ^4J=2.2 Hz); 3.13–2.87 (2H, m); 2.99 (1H, d, ^2J=13.4 Hz); 2.81 (1H, d, ^2J=13.4 Hz); 2.38–2.012 (2H, m); 2.31 (3H, s); 2.08 (6H, s); 1.04 (3H, s). ^{13}C NMR (50 MHz, $CDCl_3$) δ 204.94; 195.42; 154.45; 107.31; 72.42; 45.59; 42.63; 39.59; 38.00; 30.69; 26.53; 26.41; 26.23. MS (EI, 70 eV) 268(0) [M$^{+\bullet}$]; 225(2), 208(1), 179(2), 149(21), 137(17), 121(2), 107(5), 95(9), 91(5), 77(4), 65(2), 43(100).

(*Z*)-dimethyl 3-((acetylthio)methylene)-4-isopropylcyclo-pentane-1,1-dicarboxylate (*Z*)-**8c**. ^{1}H NMR ($CDCl_3$, 200 MHz): δ 6.26 (1H, ddd, ^4J=4.8 Hz, ^4J=2.4 Hz, ^4J∼0 Hz); 3.70 (3H, s); 3.72 (3H, s); 2.99 (1H, *br* d, ^2J=18 Hz); 2.35 (3H, s); 2.31–2.77 (3H, m); 1.86–2.16 (2H, m); 0.95 (3H, d, *J*=6.8 Hz); 0.81 (3H, d, *J*=6.8 Hz). ^{13}C NMR (50 MHz, $CDCl_3$) δ 192.21; 171.91; 171.87; 145.99; 108.74; 58.53; 53.01; 52.96; 49.61; 40.35; 34.70; 30.61; 29.66; 21.29; 16.90. MS (EI, 70 eV). HRMS calculated for $C_{19}H_{23}O_5S$ (MH^+) 315.1259; found 315.1266. Δ=2.2 ppm.

(*Z*)-Dimethyl 3-((acetylthio)methylene)-4-ethylcyclopentane-1,1-dicarboxylate (*Z*)-**9c**. ^{1}H NMR ($CDCl_3$, 200 MHz): δ 6.29 (1H, ddd, ^4J=4.6 Hz, ^4J=2.2 Hz, ^4J∼0 Hz); 3.72 (6H, s); 2.77–3.04 (2H, m); 2.49–2.67 (2H, m); 2.36 (3H, s); 1.69–1.94 (2H, m); 1.24–1.42 (1H, m); 0.93 (3H, t, *J*=7.2 Hz). ^{13}C NMR (50 MHz, $CDCl_3$) δ 192.11; 171.94; 171.92; 146.87; 108.15; 77.80; 77.16; 76.52; 58.49; 53.01; 52.95; 45.23; 39.70; 39.61; 30.61; 26.35; 11.69. MS (EI, 70 eV) 300(1) [M$^{+\bullet}$], 269(2), 225(15), 198(29), 165(51), 139(25), 105(27), 77(13), 59(32), 43(100). HRMS calculated for $C_{14}H_{21}O_5S$ (MH^+) 301.1110; found 301.1117. Δ=2.3 ppm.

(*E*)-Dimethyl 3-((acetylthio)methylene)octahydro-1H-indene-1;1-dicarboxylate (*E*)-**10c** (1 dia: cis fusion). ^{1}H NMR ($CDCl_3$, 200 MHz): δ 6.22 (1H, ddd, ^4J=5.4 Hz, ^4J=2.6 Hz, ^4J∼0 Hz); 3.96 (3H, s); 3.96 (3H, s); 3.24 (1H, ddd, ^2J=19 Hz, ^4J=2.6 Hz, ^4J=2.6 Hz); 3.00–2.85 (1H, m); 2.64–2.79 (1H, m); 2.74 (1H, *br* d, *J*=18 Hz); 2.36 (3H, s); 2.02 (1H, *br* d, *J*=14.2 Hz); 1.54–1.82 (3H, m); 1.04–1.33(3H, m); 0.69–0.89 (1H, m). ^{13}C NMR (50 MHz, $CDCl_3$) δ 192.24; 171.94; 169.98; 144.38; 107.50; 62.19; 52.92; 52.68; 45.13; 43.98; 37.00; 30.62; 24.94; 24.47; 24.27; 20.39. MS (EI; 70 eV) 328(0) [M$^{+\bullet}$]; 295(1); 250(19); 218(13); 191(36); 190(49); 165(12); 131(42); 115(5); 105(13); 91(25); 77(10); 59(24); 41(100). HRMS calculated for $C_{16}H_{23}O_5S$ (MH^+) 326.1266; found 327.1272. Δ=1.8 ppm.

(*E*)-dimethyl 3-((acetylthio)methylene)-4-(6-methylhept-5-en-2-yl)cyclopentane-1,1-dicarboxylate (*E*)-**11c** (2 diastereomers 1:1). ^{1}H NMR ($CDCl_3$, 200 MHz): δ 6.22–6.28 (2H, m); 4.97–5.17 (2H, m); 3.72 (6H,s); 3.71 (6H, s); 3.00 (2H, br d, 2*J*=17.6 Hz); 2.72 (2H, br d, 2*J*=17.8 Hz); 2.35 (6H, s); 1.67 (6H, s); 1.58 (6H, s); 1.20–2.95 (16H, m); 0.95 (3H, d, *J*=6.8 Hz); 0.79 (3H, d, *J*=6.6 Hz). ^{13}C NMR (50 MHz, $CDCl_3$) δ 192.22; 191.98; 171.86; 146.13; 145.54; 131.80; 131.71; 124.53; 124.38; 108.74; 108.26; 58.53; 52.99; 52.94; 49.53; 47.72; 40.54; 40.50; 35.81; 35.40; 34.22; 34.06; 33.75; 31.78; 30.60; 26.22; 26.02; 25.81; 25.76; 18.08; 17.74; 13.96. MS (EI, 70 eV) 382(1) [M+•]; 339(6), 306(3), 247(7), 203(5), 187(7), 169(12), 137(19), 109(17), 82(43), 69(67), 43(100), 41(79). HRMS calculated for $C_{19}H_{23}O_5S$ (MH+) 382.1814; found 382.1804. Δ=2.6 ppm.

(*Z*)-S-((4-benzyl-1-tosylpyrrolidin-3-ylidene)methyl) ethanethioate (*Z*)-**12c**. White solid, mp=108.1 °C. ^{1}H NMR ($CDCl_3$, 200 MHz): δ 2.37 (3H, s); 2.44 (3H, s); 2.56 (2H, dd, 2*J*=14 Hz, *J*=8 Hz); 2.85–3.10 (3H, m); 3.12–3.29 (1H, m); 3.64–3.87 (2H, br m); 6.27–6.38 (1H, br m); 7.11 (2H, d, *J*=6.4 Hz), 7.20–7.48 (5H, m); 7.67 (2H, d,=8.2 Hz). ^{13}C NMR (50 MHz, $CDCl_3$) δ 191.08; 144.00; 142.07; 138.67; 132.48; 129.88; 128.89; 128.75; 127.91; 126.74; 109.80; 52.85; 51.29; 45.68; 38.91; 30.68; 21.65. MS (EI, 70 eV) 401(0.22) [M+•]; 358(2), 326(18), 310(6), 268(2), 234(26), 204(3), 170(9), 155(19), 143(7), 112(15), 91(100), 80(13), 65(15), 43(45). HRMS calculated for $C_{21}H_{24}NO_3S_2$ (MH+) 402.1198; found 402.1189. Δ=2.2 ppm.

Diethyl 2-(3-(acetylthio)-2-methylpropyl)malonate **13d**. ^{1}H NMR ($CDCl_3$, 200 MHz): δ 4.19 (4H, q, *J*=7 Hz); 3.45 (1H, dd, *J*=8 Hz, *J*=6 Hz); 2.86 (2H, m); 2.32 (3H, s); 2.02 (1H, m); 1.76 (2H, m); 1.26 (6H, t, *J*=7 Hz); 0.96 (3H, d, *J*=6 Hz). ^{13}C NMR (50 MHz, $CDCl_3$) δ 195.56; 169.54; 169.35; 61.56; 61.52; 49.98; 35.49; 34.63; 31.52; 30.72; 18.92; 14.15(2). MS (EI, 70 eV) 290(0) [M$^{+\bullet}$]; 247(30), 229(2), 203(25), 173(69), 155(14), 145(11), 127(29), 101(19), 99(20), 87(9), 73(9), 67(7), 55(25), 43(100).

(*E*/*Z*)-Dimethyl 2-(3-(acetylthio)allyl)malonate **14d**. ^{1}H NMR ($CDCl_3$, 200 MHz): δ 6.66 (1H, d, 3JZ=10 Hz); 6.57 (1H, d, 3JE=16 Hz); 5.90–5.60 (2H, m); 3.74 (12H, s); 3.47 (2H, t, *J*=7 Hz); 2.80–2.55 (4H, m); 2.39 (3H, s); 2.33 (3H, s). ^{13}C NMR (50 MHz, $CDCl_3$) δ 193.04 (2), 191.59 (2), 169.02, 168.99, 129.80, 127.42, 120.39, 120.24, 52.78 (2), 51.28, 50.72, 32.38, 30.96 (2), 30.46 (2), 29.76. MS (EI, 70 eV) 246(1) [M$^{+\bullet}$]; 204(5), 173(7), 171(14), 145(5), 113(15), 111(20), 100(2), 85(100), 72(4), 59(9), 65(11), 43(100).

Acknowledgements

This work was supported by the University Nice Sophia Antipolis, the CNRS, and the ANR program CD2I (Nanocausys project, grant number 12-CDII-0010-02). We are grateful to Dr. A. Barats for ICP-MS analysis, Dr. L. Feray for fruitful discussion on radical mechanisms, and Ms C. Diefoldo for her technical assistance.

Supplementary data

Experimental details, characterization data, and ^{1}H, ^{13}C NMR and MS spectra of the cyclized products, computational details. Supplementary data related to this article can be found at http://dx.doi.org/10.1016/j.tet.2014.10.077.

References and notes

1. Anastas, P.; Warner, J. *Green Chemistry: Theory and Practice*; Oxford University: Oxford, UK, 1998.
2. de Almeida, M. P.; Carabineiro, S. A. C. *ChemCatChem* **2012**, *4*, 18–29.
3. Huang, W.; Liu, J. H.-C.; Alayoglu, P.; Li, Y.; Witham, C. A.; Tsung, C.-K.; Toste, F. D.; Somorjai, G. A. *J. Am. Chem. Soc.* **2010**, *132*, 16771–16773.
4. Witham, C. A.; Huang, W.; Tsung, C.-K.; Kuhn, J. N.; Somorjai, G. A.; Toste, F. D. *Nat. Chem.* **2010**, *2*, 36–41.
5. MacQuarrie, D. J. In *Heterogenized Homogeneous Catalysts for Fine Chemicals Production*; Barbaro, P., Liguiro, F., Eds.; Springer: New York, NY, 2010; pp 1–35.
6. *Nanoparticles and Catalysis*; Astruc, D., Ed.; Wiley-VCH GmbH & KGaA, Weinheim: 2008.
7. Stratakis, M.; Garcia, H. *Chem. Rev.* **2012**, *112*, 4469–4506.
8. Pagliaro, M.; Pandarus, V.; Ciriminna, R.; Béland, F.; Demma Carà, P. *ChemCatChem* **2012**, *4*, 432–445.
9. Ranu, B. C.; Dey, R.; Chatterjee, T.; Ahammed, S. *ChemSusChem* **2012**, *5*, 22–44.
10. Heshmatpour, F.; Abazari, R.; Balalaie, S. *Tetrahedron* **2012**, *68*, 3001–3011.
11. Heugebaert, T. S. A.; De Corte, S.; Sabbe, T.; Hennebel, T.; Verstraete, W.; Boon, N.; Stevens, C. V. *Tetrahedron Lett.* **2012**, *53*, 1410–1412.
12. Gryparis, C.; Efe, C.; Raptis, C.; Lykakis, I. N.; Stratakis, M. *Org. Lett.* **2012**, *14*, 2956–2959.
13. Michelet, V.; Toullec, P. Y.; Genêt, J.-P. *Angew. Chem., Int. Ed.* **2008**, *47*, 4268–4315.
14. Fürstner, A.; Davies, P. W. *Angew. Chem., Int. Ed.* **2007**, *46*, 3410–3449.
15. Buzas, A. K.; Istrate, F. M.; Gagosz, F. *Angew. Chem., Int. Ed.* **2007**, *46*, 1141–1144.
16. Amijs, C. H. M.; Lopez-Carrillo, V.; Raducan, M.; Perez-Galan, P.; Ferrer, C.; Echavarren, A. M. *J. Org. Chem.* **2008**, *73*, 7721–7730.
17. Toullec, P. Y.; Genin, E.; Leseurre, L.; Genêt, J.-P.; Michelet, V. *Angew. Chem., Int. Ed.* **2006**, *45*, 7427–7430.
18. Nakamura, I.; Sato, T.; Yamamoto, Y. *Angew. Chem., Int. Ed.* **2006**, *45*, 4473–4475.
19. Brouwer, C.; Rahaman, R.; He, C. *Synlett* **2007**, 1785–1789.
20. Nakamura, I.; Sato, T.; Terada, M.; Yamamoto, Y. *Org. Lett.* **2008**, *10*, 2649–2651.
21. Heugebaert, T. S. A.; Vervaecke, L. P. D.; Stevens, C. V. *Org. Biomol. Chem.* **2011**, *9*, 4791–4794.

22. Corma, A.; González-Arellano, C.; Iglesias, M.; Sánchez, F. *Appl. Catal., A* **2010**, *375*, 49–54.
23. Broka, C. A.; Reichert, D. E. C. *Tetrahedron Lett.* **1987**, *28*, 1503–1505.
24. Taniguchi, T.; Fujii, T.; Idota, A.; Ishibashi, H. *Org. Lett.* **2009**, *11*, 3298–3301.
25. Mudd, R. J.; Young, P. C.; Jordan-Hore, J. A.; Rosair, G. M.; Lee, A.-L. *J. Org. Chem.* **2012**, *77*, 7633–7639.
26. Mondal, S.; Gold, B.; Mohamed, R. K.; Phan, H.; Alabugin, I. V. *J. Org. Chem.* **2014**, *79*, 7491–7501.
27. Mondal, S.; Mohamed, R. K.; Manoharan, M.; Phan, H.; Alabugin, I. V. *Org. Lett.* **2013**, *15*, 5650–5653.
28. Leyva-Pérez, A.; Oliver-Meseguer, J.; Cabrero-Antonino, J. R.; Rubio-Marquès, P.; Serna, P.; Al-Resayes, S. I.; Corma, A. *ACS Catal.* **2013**, *3*, 1865–1873.
29. bin Saiman, M. I.; Brett, G. L.; Tiruvalam, R.; Forde, M. M.; Sharples, K.; Thetford, A.; Jenkins, R. L.; Dimitratos, N.; Lopez-Sanchez, J. A.; Murphy, D. M.; Bethell, D.; Willock, D. J.; Taylor, S. H.; Knight, D. W.; Kiely, C. J.; Hutchings, G. J. *Angew. Chem., Int. Ed.* **2012**, *51*, 5981–5985.
30. Gates, B. C. *Chem. Commun.* **2013**, 7876–7877.
31. Edwards, J. K.; Solsona, B. E.; Landon, P.; Carley, A. F.; Herzing, A.; Kiely, C. J.; Hutchings, G. J. *J. Catal.* **2005**, *236*, 69–79.
32. Dimitratos, N.; Lopez-Sanchez, J. A.; Anthonykutty, J. M.; Brett, G.; Carley, A. F.; Tiruvalam, R. C.; Herzing, A. A.; Kiely, C. J.; Knight, D. W.; Hutchings, G. J. *Phys. Chem. Chem. Phys.* **2009**, *11*, 4952–4961.
33. Wille, U. *Chem. Rev.* **2013**, *113*, 813–853.
34. Biermann, U.; Butte, W.; Koch, R.; Fokou, P. A.; Türünç, O.; Meier, M. A. R.; Metzger, J. O. *Chem.—Eur. J.* **2012**, *18*, 8201–8207.
35. Tan, K. J.; White, J. M.; Wille, U. *Eur. J. Org. Chem.* **2010**, *2010*, 4902–4911.
36. Dénès, F.; Pichowicz, M.; Povie, G.; Renaud, P. *Chem. Rev.* **2014**, *114*, 2587–2693.
37. Godeau, J.; Olivero, S.; Antoniotti, S.; Duñach, E. *Org. Lett.* **2011**, *13*, 3320–3323.
38. Trost, B. M.; Dumas, J. *Tetrahedron Lett.* **1993**, *34*, 19–22.